Inorganic Chemistry

ARTICLE

pubs.acs.org/IC

$Ca_{10}Ge_{16}B_6O_{51}$ and $Cd_{12}Ge_{17}B_8O_{58}$: Two Types of New 3D Frameworks Based on BO_4 Tetrahedra and 1D $[Ge_4O_{12}]_n$ Chains

Xiang Xu, Chun-Li Hu, Fan Kong, Jian-Han Zhang, and Jiang-Gao Mao*

State Key Laboratory of Structural Chemistry, Fujian Institute of Research on the Structure of Matter, Chinese Academy of Sciences, Fuzhou 350002, P. R. China

Supporting Information

ABSTRACT: Two new acentric borogermanates, $Ca_{10}Ge_{16}B_6O_{51}$ (*Pba*2) and $Cd_{12}Ge_{17}B_8O_{58}$ ($P\bar{4}$), have been successfully synthesized by high-temperature solid-state reactions of $CaCO_3$ (or $CdCO_3$), GeO_2, and H_3BO_3. Both structures display the same one-dimensional (1D) $[Ge_4O_{12}]_n$ chains composed of GeO_4 tetrahedra and GeO_6 octahedra. In $Ca_{10}Ge_{16}B_6O_{51}$, neighboring 1D $[Ge_4O_{12}]_n$ chains are condensed into a two-dimensional (2D) $[Ge_4O_{10.75}]_n$ layer via corner sharing, and such layers are further interconnected by "isolated" BO_4 tetrahedra and B_2O_7 dimers into a three-dimensional (3D) framework, forming 1D tunnels of 5-, 6-, and 7-MRs along the *c* axis that are occupied by Ca^{2+} cations. In $Cd_{12}Ge_{17}B_8O_{58}$, neighboring 1D $[Ge_4O_{12}]_n$ chains are interconnected into a $[Ge_4O_{10.5}]_n$ open framework via corner sharing with large pores filled by big $[Ge(B_2O_7)_4]^{28-}$ clusters, leading to formation of three types of 1D tunnels of 5-, 6-, and 7-membered rings (MRs) along the *c* axis which are occupied by the Cd^{2+} cations. Both compounds are transparent in the range of 0.3−6.67 μm and exhibit very weak SHG responses.

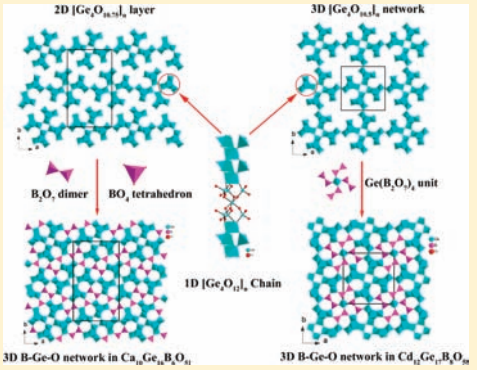

INTRODUCTION

Recently, metal borogermanates have attracted considerable research interest due to their abundant structure types derived from the flexible coordination geometries for both Ge and B atoms. A series of organically templated borogermanates has been reported by the Zou and Yang groups,[1,2] some of which exhibit various new zeolite-type frameworks. However, the presence of water molecules or organic templates in their structures would reduce their thermal stability and limit their practical use. On the other hand, a series of new alkali metal and rare-earth borogermanates has also been synthesized during the past decade.[3−10] Some of them also display a number of interesting open-framework structures, for example, $KBGe_2O_6$[3a] exhibits a chiral zeotype framework with seven-membered ring (7-MR) channels and $NH_4[BGe_3O_8]$[6b] features a three-dimensional (3D) open framework with one-dimensional (1D) 10-membered ring (10-MR) channels. More interestingly, some of them exhibit special physical properties such as second-harmonic generation (SHG) and luminescence, for example, $K_2GeB_4O_9 \cdot 2H_2O$ and $CsGeB_3O_7$ exhibit moderate SHG responses of 2.0 and 1.5 × KDP (KH_2PO_4), respectively,[3b,4] and $Eu_2GeB_2O_8$ and $Tb_2GeB_2O_8$ emit strong red and green light, respectively.[8a]

As for the alkaline-earth and transition-metal borogermanates, only $Ni_5GeB_2O_{10}$,[11] $Ba_3[Ge_2B_7O_{16}(OH)_2](OH)(H_2O)$, and $Ba_3Ge_2B_6O_{16}$[12] have been structurally characterized. $Ni_5GeB_2O_{10}$ features a layered $[NiGeB_2O_{10}]^{8-}$ architecture built of 1D chains of edge-sharing $Ge(Ni)O_6$ octahedra that are further bridged by BO_3 triangles; mixing of Ni and Ge sites also occurred. $Ba_3[Ge_2B_7O_{16}(OH)_2](OH)(H_2O)$ and $Ba_3Ge_2B_6O_{16}$ feature two types of anionic open frameworks based on two types of polymeric borate units ($B_7O_{16}(OH)_2$ and B_6O_{16}) interconnected by GeO_4 tetrahedra. The different coordination geometries and ionic radii of alkaline-earth and transition metals from those of the alkali and rare-earth elements may lead to metal borogermanates with different structures and physical properties. Therefore, we started a research program to explore alkaline-earth and transition-metal borogermanates systematically. Our research efforts in this aspect led to the discovery of two new borogermanates with noncentrosymmetric (NCS) structure, namely, $Ca_{10}Ge_{16}B_6O_{51}$ and $Cd_{12}Ge_{17}B_8O_{58}$. Herein, we report their syntheses, crystal structures, as well as optical properties.

EXPERIMENTAL SECTION

Materials and Methods. All of the chemicals were analytically pure from commercial sources and used without further purification. IR spectra were recorded on a Magna 750 FT-IR spectrometer as KBr pellets in the range of 4000−400 cm^{-1} with a resolution of 2 cm^{-1} at room temperature. Microprobe elemental analyses were performed on a field emission scanning electron microscope (FESEM, JSM6700F) equipped with an energy-dispersive X-ray spectroscope (EDS, Oxford INCA). X-ray powder diffraction (XRD) patterns were collected on a Rigaku MiniFlex II diffractometer using Cu Kα radiation in the angular range of $2\theta = 5-65°$ with a step size of 0.02°. Optical diffuse reflectance and UV spectra were measured at room temperature with a Perkin-Elmer Lambda 900 UV−vis−NIR spectrophotometer. A $BaSO_4$ plate

Received: April 20, 2011
Published: August 17, 2011

Table 1. Summary of Crystal Data and Structure Refinements of $Ca_{10}Ge_{16}B_6O_{51}$ and $Cd_{12}Ge_{17}B_8O_{58}$

formula	$Ca_{10}Ge_{16}B_6O_{51}$	$Cd_{12}Ge_{17}B_8O_{58}$
fw	2443.10	3597.31
cryst syst	orthorhombic	tetragonal
space group	*Pba*2	$P\bar{4}$
a, Å	15.119(8)	14.928(2)
b, Å	26.34(1)	14.928(2)
c, Å	4.717(2)	4.698(1)
V, Å^3	1877.0(2)	1046.8(3)
Z	2	1
D_{calcd}, g cm^{-3}	4.323	5.707
μ (Mo Kα), mm^{-1}	14.137	18.109
GOF on F^2	1.162	0.988
Flack factor	−0.01(2)	0.02(1)
R1, wR2 ($I > 2\sigma(I)$)[a]	0.0329, 0.0698	0.0145, 0.0297
R1, wR2 (all data)	0.0377, 0.0726	0.0167, 0.0301

[a] $R1 = \Sigma||F_c| - |F_o||/\Sigma|F_o|$; $wR_2 = \{\Sigma w[(F_o)^2 - (F_c)^2]^2/\Sigma w[(F_o)^2]^2\}^{1/2}$.

was used as a standard (100% reflectance). The absorption spectrum was calculated from reflectance spectra using the Kubelka−Munk function: $\alpha/S = (1 - R)^2/2R$, where α is the absorption coefficient, *S* is the scattering coefficient which is practically wavelength independent when the particle size is larger than 5 μm, and *R* is the reflectance.[13] Thermogravimetric analyses (TGA) were carried out with a NETZCH STA449C unit at a heating rate of 15 °C min^{-1} under N_2 atmosphere, and differential scanning calorimetry (DSC) analyses were performed under N_2 on a NETZSCH DTA404PC unit at rate of 15 °C min^{-1} including the heating and cooling processes. Measurements of the powder frequency-doubling effect were carried out on the sieved sample (70−100 mesh) by means of the modified method of Kurtz and Perry.[14] The fundament wavelength is 1064 nm generated by a Q-switched Nd:YAG laser. Sieved KDP (KH_2PO_4) sample in the same size range was used as a reference.

Syntheses of $Ca_{10}Ge_{16}B_6O_{51}$ and $Cd_{12}Ge_{17}B_8O_{58}$. Single crystals of the two compounds were obtained by high-temperature solid-state reactions of $CaCO_3$ (or $CdCO_3$), GeO_2, and H_3BO_3. The mixture of $CaCO_3$ or $CdCO_3$, GeO_2, H_3BO_3 was ground in an agate mortar and transferred to platinum crucibles. The loaded compositions are as follows: $CaCO_3$ (8 mmol, 0.801 g), GeO_2 (10 mmol, 1.046 g), and H_3BO_3 (16 mmol, 0.989 g) for $Ca_{10}Ge_{16}B_6O_{51}$; $CdCO_3$ (8 mmol, 1.379 g), GeO_2 (4 mmol, 0.418 g), and H_3BO_3 (16 mmol, 0.989 g) for $Cd_{12}Ge_{17}B_8O_{58}$. For $Ca_{10}Ge_{16}B_6O_{51}$, the mixture was heated at 1080 °C for 20 h and then cooled to 900 °C at a rate of 3 °C h^{-}before the furnace was switched off, whereas for $Cd_{12}Ge_{17}B_8O_{58}$ the mixture was heated at 980 °C for 10 h and then cooled to 550 °C at a rate of 3 °C h^{-1}. The average atomic ratios of Ca:Ge and Cd:Ge determined by energy-dispersive spectrometry (EDS) on several single crystals are 0.62:1 and 0.63:1, respectively, which are in good agreement with those determined from single-crystal X-ray structure analyses. After proper structural analyses, pure polycrystalline samples of both compounds were obtained quantitatively by the solid-state reactions of a $CaO/GeO_2/H_3BO_3$ mixture in a molar ratio of 5:8:3 for $Ca_{10}Ge_{16}B_6O_{51}$ and $CdCO_3/GeO_2/H_3BO_3$ mixture in a molar ratio of 12:17:8 for $Cd_{12}Ge_{17}B_8O_{58}$. CaO was sintered in a muffle furnace at 800 °C for 12 h prior to use in order to remove absorbed water and carbon dioxide. The initial mixture was ground thoroughly in an agate motor and then heated at 850 °C for 2 h for both compounds, 1050 °C for $Ca_{10}Ge_{16}B_6O_{51}$, and 900 °C for $Cd_{12}Ge_{17}B_8O_{58}$ for 10 days. It was reground after heat treatment at 850 °C. Their purities were confirmed by power XRD diffraction studies (Figures S1 and S2, Supporting Information). In addition, a

Table 2. Important Bond Lengths (Å) for $Ca_{10}Ge_{16}B_6O_{51}$ and $Cd_{12}Ge_{17}B_8O_{58}$[a]

$Ca_{10}Ge_{16}B_6O_{51}$			
Ge(1)−O(11)	1.754(5)	Ge(1)−O(12)	1.758(5)
Ge(1)−O(4)	1.779(5)	Ge(1)−O(19)#1	1.766(5)
Ge(2)−O(11)	1.853(5)	Ge(2)−O(2)#2	1.872(5)
Ge(2)−O(1)	1.888(5)	Ge(2)−O(12)#2	1.874(5)
Ge(2)−O(3)	1.890(5)	Ge(2)−O(7)#2	1.879(5)
Ge(3)−O(3)	1.735(5)	Ge(3)−O(2)	1.745(5)
Ge(3)−O(9)	1.762(5)	Ge(3)−O(21)	1.762(5)
Ge(4)−O(5)#3	1.874(5)	Ge(4)−O(14)#1	1.874(5)
Ge(4)−O(13)	1.881(5)	Ge(4)−O(16)	1.881(5)
Ge(4)−O(6)#1	1.883(5)	Ge(4)−O(22)#4	1.914(5)
Ge(5)−O(7)	1.727(5)	Ge(5)−O(8)	1.740(5)
Ge(5)−O(1)	1.754(5)	Ge(5)−O(18)	1.771(5)
Ge(6)−O(19)	1.756(5)	Ge(6)−O(13)	1.758(5)
Ge(6)−O(4)#3	1.759(5)	Ge(6)−O(14)	1.760(5)
Ge(7)−O(20)	1.742(5)	Ge(7)−O(16)	1.748(5)
Ge(7)−O(6)	1.754(5)	Ge(7)−O(17)	1.769(5)
Ge(8)−O(5)	1.742(5)	Ge(8)−O(15)	1.757(5)
Ge(8)−O(22)	1.762(5)	Ge(8)−O(10)	1.801(3)
B(1)−O(23)	1.33(1)	B(1)−O(18)	1.536(9)
B(1)−O(9)#5	1.559(8)	B(1)−O(17)#1	1.589(8)
B(2)−O(24)	1.38(1)	B(2)−O(25)	1.477(8)
B(2)−O(8)	1.530(8)	B(2)−O(20)#6	1.549(8)
B(3)−O(26)	1.38(1)	B(3)−O(25)#7	1.472(8)
B(3)−O(21)	1.515(8)	B(3)−O(15)	1.602(8)
$Cd_{12}Ge_{17}B_8O_{58}$			
Ge(1)−O(10)	1.733(3)	Ge(1)−O(10)#1	1.733(3)
Ge(1)−O(10)#2	1.733(3)	Ge(1)−O(10)#3	1.733(3)
Ge(2)−O(9)	1.741(3)	Ge(2)−O(15)	1.758(3)
Ge(2)−O(5)	1.761(3)	Ge(2)−O(8)	1.779(2)
Ge(3)−O(14)	1.747(3)	Ge(3)−O(7)	1.747(3)
Ge(3)−O(4)	1.752(3)	Ge(3)−O(6)	1.752(3)
Ge(4)−O(13)	1.750(3)	Ge(4)−O(12)#4	1.759(3)
Ge(4)−O(12)	1.763(3)	Ge(4)−O(3)	1.775(3)
Ge(5)−O(13)#5	1.857(3)	Ge(5)−O(5)#5	1.859(3)
Ge(5)−O(6)	1.861(3)	Ge(5)−O(3)	1.881(3)
Ge(5)−O(4)#5	1.893(3)	Ge(5)−O(15)	1.896(3)
B(1)−O(11)	1.413(7)	B(1)−O(1)#5	1.466(5)
B(1)−O(14)#6	1.523(5)	B(1)−O(9)	1.526(5)
B(2)−O(2)#7	1.392(7)	B(2)−O(1)#8	1.471(5)
B(2)−O(7)#9	1.514(5)	B(2)−O(10)	1.553(5)

[a] Symmetry transformations used to generate equivalent atoms. For $Ca_{10}Ge_{16}B_6O_{51}$: #1 *x*, *y*, *z* + 1; #2 *x*, *y*, *z* − 1; #3 −*x* + 1, −*y*, *z* − 1; #4 −*x* + 1, −*y*, *z*; #5 *x* − 1/2, −*y* + 1/2, *z*; #6 *x* + 1/2, −*y* + 1/2, *z* + 1; #7 *x* + 1/2, −*y* + 1/2, *z*. For $Cd_{12}Ge_{17}B_8O_{58}$: #1 −*y*, *x*, −*z* + 2; #2 *y*, −*x*, −*z* + 2; #3 −*x*, −*y*, *z*; #4 *y*, −*x* + 1, −*z* + 2; #5 −*y* + 1, *x*, −*z* + 2; #6 −*y* + 1, *x*, −*z* + 2; #7 *y*, −*x*, −*z* + 1; #8 −*x*, −*y*, *z* + 1; #9 *x*, *y* − 1, *z*.

whole-powder profile fitting procedure using the program GSAS by the Rieltveld refinements was performed.[15] Nine profile parameters were used for refinements, and unit cell parameters are refined with atomic positions fixed. Details of XRD pattern refinements are summarized in Table S1, Supporting Information. As these plots from the Rieltveld refinements fit well with the measurement power XRD diffraction patterns and the lattice parameters suggested by these procedures are

dx.doi.org/10.1021/ic2008254 |*Inorg. Chem.* 2011, 50, 8861–8868

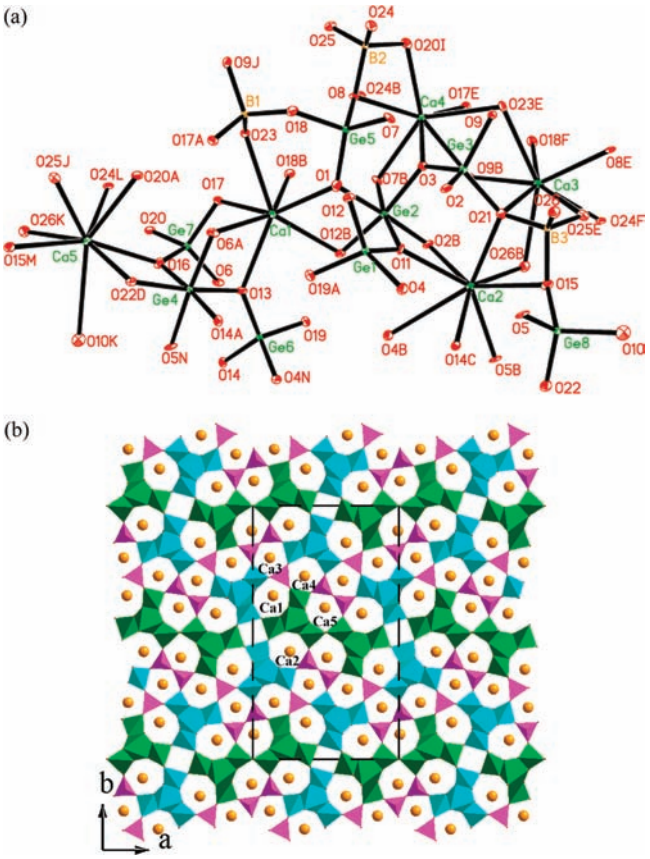

Figure 1. (a) ORTEP representation of the selected unit in $Ca_{10}Ge_{16}B_6O_{51}$. The thermal ellipsoids are drawn at 50% probability. Symmetry codes for the generated atoms: (A) $x, y, z+1$; (B) $x, y, z-1$; (C) $-x+1, -y, z+1$; (D) $-x+1, -y, z$; (E) $x+1/2, -y+1/2, z$; (F) $x+1/2, -y+1/2, z-1$; (I) $x+1/2, -y+1/2, z+1$; (J) $x-1/2, -y+1/2, z$; (K) $x-1, y, z-1$; (L) $x-1/2, -y+1/2, z-1$; (M) $x-1, y, z$; (N) $-x+1, -y, z-1$. (b) View of the structure of $Ca_{10}Ge_{16}B_6O_{51}$ along the c axis. The Ge−O polyhedra and BO_4 tetrahedra are shaded in cyan (or green for those of double Ge−O chain) and pink, respectively.

very approximate to these obtained by single-crystal X-ray diffraction, the purities of synthetic sample were further confirmed (Figures S3 and S4, Supporting Information). Efforts to synthesize the magnesium(II), strontium(II), and zinc(II) borogermanate by using a similar technique were tried but unsuccessful.

X-ray Crystallography. X-ray diffraction data collection for the two compounds was performed on a Rigaku SATURN 70 CCD diffractometer equipped with graphite-monochromated Mo Kα radiation ($\lambda = 0.71073$ Å) at 293 K. The data sets were corrected for Lorentz and polarization factors as well as absorption by the multiscan method.[16a] The two structure were solved by direct methods and refined by full-matrix least-squares fitting on F^2 using SHELX-97.[16b] All atoms were refined with anisotropic thermal parameters except for B(1), B(2), and B(3) in $Ca_{10}Ge_{16}B_6O_{51}$, which were refined with equal isotropic thermal parameters. If this constraint is not applied, the displacement parameters for B(3) will be abnormally small or these three atoms display 2D-like thermal ellipsoids if they are refined anistropically which may be due to the poor quality of the data set. Both the refined Flack factors of −0.01(2) for $Ca_{10}Ge_{16}B_6O_{51}$ and 0.02(1) for $Cd_{12}Ge_{17}B_8O_{58}$ are close to zero, confirming the correctness of the absolute structures. The structures were also checked for possible missing symmetry with PLATON.[16c] Crystallographic data and structural refinements are summarized in Table 1. Important bond distances are listed in Table 2. More details on the crystallographic studies as well as atomic displacement parameters are given in the Supporting Information.

RESULTS AND DISCUSSION

Crystal Structure Descriptions. Explorations of new alkaline-earth and transition-metal borogermanates led to two new non-centrosymmetric(NCS) compounds, namely, $Ca_{10}Ge_{16}B_6O_{51}$ and $Cd_{12}Ge_{17}B_8O_{58}$. Both of them are germanium rich rather than boron rich as in most metal borogermanates reported previously. It is interesting to note that both structures are based on the 1D $[Ge_4O_{12}]_n$ chains and BO_4 polyhedra.

$Ca_{10}Ge_{16}B_6O_{51}$ crystallizes in the polar space group *Pba*2 (No. 32). Its structure features a 3D B−Ge−O network composed $[Ge_4O_{10.75}]_n$ layers which are further bridged by the BO_4 tetrahedra and B_2O_7 dimers, forming the 1D tunnels of 5-, 6-, and 7-MR along the c axis that are occupied by the Ca^{2+} ions (Figure 1b). The asymmetric unit of $Ca_{10}Ge_{16}B_6O_{51}$ contains eight Ge, three B, and five Ca atoms (Figure 1a). Ge(2) and Ge(4) are octahedrally coordinated by six O atoms, whereas the other Ge atoms are tetrahedrally coordinated by four O atoms. As a consequence, the Ge−O bond distances fall into two categories: 1.727(5)−1.801(3) Å for GeO_4 tetrahedra and 1.853(5)−1.914 (5) Å for GeO_6 octahedra. All B atoms are in a tetrahedral geometry that is distorted from the regular tetrahedron with the ideal T_d symmetry and the B−O bond distances are in the range of 1.33(1)−1.602(9) Å. Obviously, the variation of B−O bond lengths is somehow large, which can be attributed to the anisotropic surrounding of the BO_4 tetrahedra. In other words, this may be due to the different connectivity fashion for each oxygen atom. Take $B(2)O_4$ tetrahedron as an example: the four oxygen atoms can be divided into three groups, O(24) is further connected with three Ca, O(25) is further connected with two Ca and one B, and O(8) and O(20) each is further connected with two Ca and one Ge. Of the five unique Ca atoms, Ca(1) is seven coordinated whereas the remaining ones are eight coordinated with Ca−O distances in the range 2.256(5)−3.023(4) Å. The bond valence sums of Ge, B, and Ca are calculated using the formula

$$V_i = \sum_j S_{ij} = \sum_j \exp\{(r_0 - r_{ij})/B\}$$

where S_{ij} is the bond valence associated with bond length r_{ij} and r_0 and B (usually 0.37) are empirically determined parameters.[17] The calculated total bond valence for Ge, B, and Ca atoms are summarized in Table 3. Results indicate that the Ge, B, and Ca atoms are in oxidation states of +4, +3, and +2 respectively.

The $Ge(1)O_4$, $Ge(3)O_4$, and $Ge(5)O_4$ tetrahedra and $Ge(2)O_6$ octahedra are interconnected via vertex sharing into 1D $[Ge_4O_{12}]_n$ chains along the c axis, so are $Ge(6)O_4$, $Ge(7)O_4$, and $Ge(8)O_4$ tetrahedra and $Ge(4)O_6$ octahedra (Figure 2a and 2b). Within each chain, a pair of GeO_6 octahedra is bridged by three GeO_4 tetrahedra. A pair of 1D chains containing Ge(4), Ge(6), Ge(7), and Ge(8) atoms form a $[Ge_4O_{11.5}]_n$ double chain via Ge(8)−O(10)−Ge(8) bridges (Figure 2b). Such double chains are further bridged by the 1D $[Ge_4O_{12}]_n$ chains of Ge(1), Ge(2), Ge(3), and Ge(5) into a 2D $[Ge_4O_{10.75}]_n$ layer parallel to the *ac* plane (Figure 2c). Each 1D chain of Ge(1), Ge(2), Ge(3), and Ge(5) is connected to two $[Ge_4O_{11.5}]_n$ double chains via Ge(1)−O(4)−Ge(6) and Ge(1)−O(19)−Ge(6), whereas each double chain is connected with four 1D $[Ge_4O_{12}]_n$ chains containing Ge(1), Ge(2), Ge(3), and Ge(5)

dx.doi.org/10.1021/ic2008254 |*Inorg. Chem.* 2011, 50, 8861–8868

via Ge(1)−O(4)−Ge(6) and Ge(1)−O(19)−Ge(6) bridges. These 2D layers are further bridged by "isolated" $B(1)O_4$ tetrahedra and B_2O_7 dimers formed by corner-sharing $B(2)O_4$ and $B(3)O_4$ tetrahedra, forming five types of 1D tunnels of one 5-MR, two 6-MR, and two 7-MR along the *c* axis in the 3D $[Ge_{16}O_{29}(B_2O_7)_2(BO_4)_2]^{20-}$ anionic structure (Figure 2d). The 5-MR filled by Ca(3) is formed by two GeO_4 and three BO_4 tetrahedra. The 6-MR filled by Ca(4) is composed of three GeO_4, one GeO_6, and two BO_4 (one "isolated" and one from a B_2O_7 dimer), whereas the 6-MR filled by Ca(5) is composed of three GeO_4, one GeO_6, and two BO_4 from a B_2O_7 dimer. The 7-MR filled by Ca(1) contains four GeO_4, two GeO_6, and one "isolated" BO_4, whereas the 7-MR occupied by Ca(2) contains four GeO_4, two GeO_6, and one BO_4 from a B_2O_7 dimer. The B−O−B bond angle is 131.1(7)°, and the Ge−O−Ge and B−O−Ge angles are ranging from 119.0(3)° to 130.0(4)° and 119.2(5)° to 131.1(7)°, respectively. These bond angles are comparable to those previously reported in related borogermanates.[1−12]

Table 3. Calculated Bond Valence Sum for $Ca_{10}Ge_{16}B_6O_{51}$ and $Cd_{12}Ge_{17}B_8O_{58}$

atom	bond valence sum	atom	bond valence sum
		$Ca_{10}Ge_{16}B_6O_{51}$	
Ge(1)	3.83	Ge(2)	4.24
Ge(3)	3.97	Ge(4)	4.15
Ge(5)	4.00	Ge(6)	3.89
Ge(7)	3.94	Ge(8)	3.82
B(1)	2.90	B(2)	3.00
B(3)	2.95	Ca(1)	2.19
Ca(2)	2.30	Ca(3)	1.82
Ca(4)	2.16	Ca(5)	2.10
		$Cd_{12}Ge_{17}B_8O_{58}$	
Ge(1)	4.17	Ge(2)	3.88
Ge(3)	3.98	Ge(4)	3.86
Ge(5)	4.27	B(1)	2.99
B(2)	3.00	Cd(1)	1.97
Cd(2)	2.05	Cd(3)	1.87

$Cd_{12}Ge_{17}B_8O_{58}$ crystallizes in the tetragonal crystal system with an acentric space group of $P\bar{4}$ (No. 81). Its structure exhibits a very complicated 3D B−Ge−O network built from a 3D $[Ge_4O_{10.5}]_n$ network based on also 1D $[Ge_4O_{12}]_n$ chains observed in $Ca_{10}Ge_{16}B_6O_{51}$ and $[Ge(B_2O_7)_4]^{28-}$ clusters, forming 1D tunnels of 5-, 6-, and 7-MRs along the *c* axis that are occupied by the Cd^{2+} cations (Figure 3b). The asymmetric unit of $Cd_{12}Ge_{17}B_8O_{58}$ contains five Ge, two B, and three Cd atoms (Figure 3a). The Ge(1) atom is located on the 4-fold axis, whereas all other atoms are in general positions. Ge(1), Ge(2), Ge(3), and Ge(4) are tetrahedrally coordinated by four O atoms with Ge−O bond distances ranging from 1.733(3) to 1.779(2) Å, whereas Ge(5) is octahedrally coordinated by six O atoms with the Ge−O bond distances ranging from 1.857(3) to 1.896(3) Å. Both B atoms are in a distorted tetrahedral geometry, and the B−O bond distances are in the range of 1.392(7)−1.553(5) Å. Similar to $Ca_{10}Ge_{16}B_6O_{51}$, the B−O bond lengths also have a large variation, which may be also due to the different coordination environment of the four oxygen atoms in a BO_4 tetrahedron. Of the three independent Cd atoms, Cd(1) and Cd(3) are seven coordinated whereas Cd(2) is octahedrally coordinated with Cd−O distances in the range 2.251(3)−2.583(3) Å. The bond valence sums of Ge, B, and Cd are calculated using the method described above (Table 3). The Ge, B, and Cd

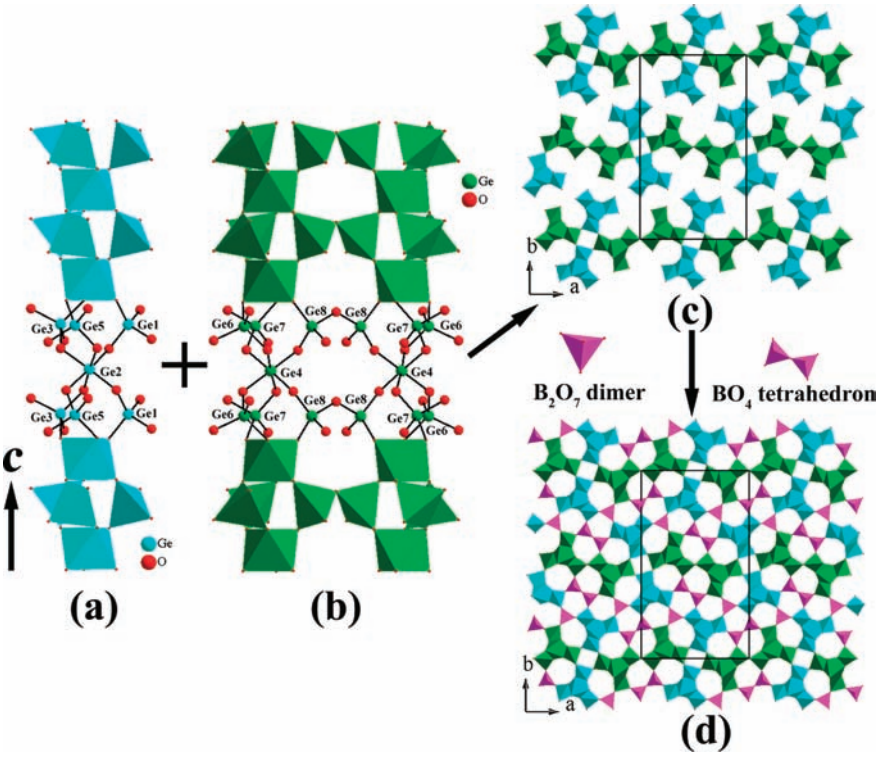

Figure 2. Scheme showing of the 1D $[Ge_4O_{12}]_n$ chain (a) and $[Ge_4O_{11.5}]_n$ double chains along the *c* axis (b) and then construction of 2D $[Ge_4O_{10.75}]_n$ layers along the *ac* plane (c) and a 3D $[Ge_{16}O_{29}(B_2O_7)_2(BO_4)_2]^{20-}$ anionic network (d) in $Ca_{10}Ge_{16}B_6O_{51}$.

dx.doi.org/10.1021/ic2008254 |*Inorg. Chem.* 2011, 50, 8861–8868

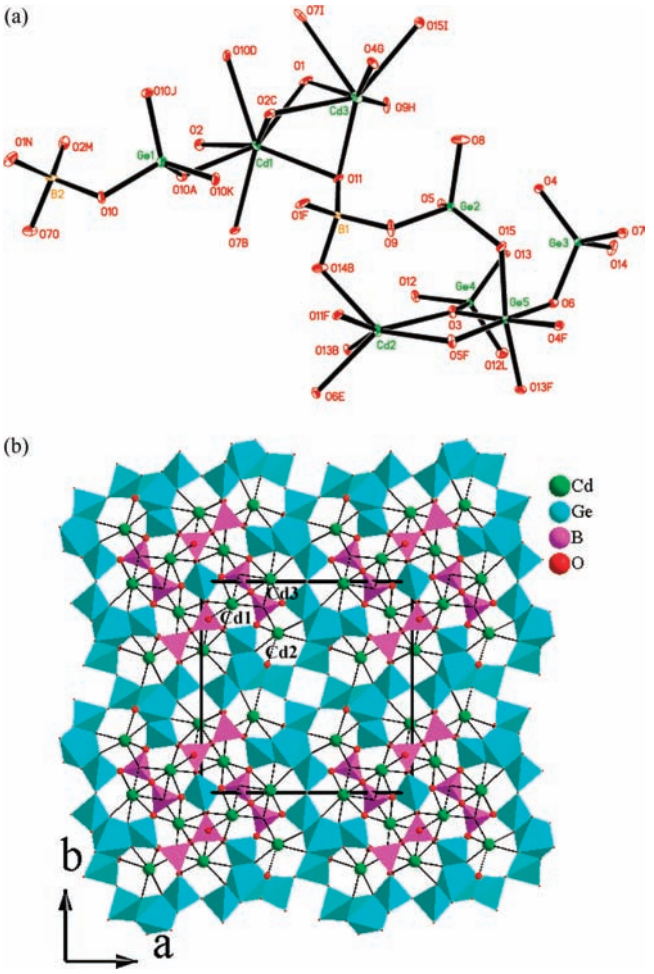

Figure 3. (a) ORTEP representation of the selected unit in $Cd_{12}Ge_{17}B_8O_{58}$. The thermal ellipsoids are drawn at 50% probability. Symmetry codes: (A) $-y, x, -z+2$; (B) $-y+1, x, -z+2$; (C) $-y, x, -z+1$; (D) $-x, -y, z-1$; (E) $-y+1, x, -z+3$; (F) $x, y, z+1$; (G) $-x, -y+1, z$; (H) $x, y, z-1$; (I) $-x, -y+1, z-1$; (J) $y, -x, -z+1$; (K) $-x, -y, z$; (L) $y, -x+1, -z+2$; (M) $y, -x, -z+1$; (N) $-x, -y, z+1$; (O) $x, y-1, z$. (b) View of the structure of $Cd_{12}Ge_{17}B_8O_{58}$ along the c axis. The Ge−O polyhedra and BO_4 tetrahedra are shaded in cyan and pink, respectively.

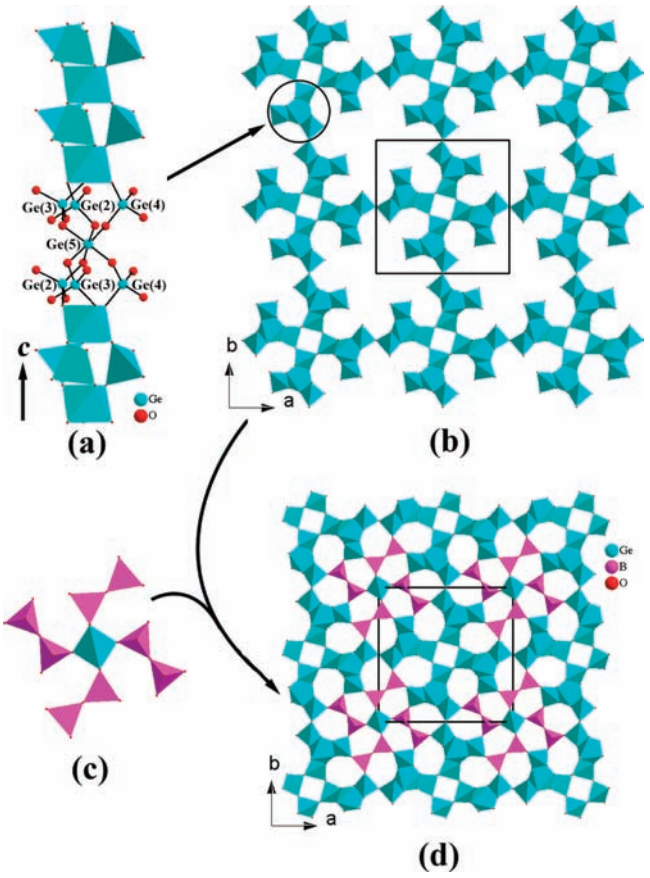

Figure 4. Scheme showing a 1D $[Ge_4O_{12}]_n$ chain (a) and construction of a 3D $[Ge_4O_{10.5}]_n$ network (b) and then a $Ge(B_2O_7)_4$ unit (c) and construction of a 3D $[Ge_{17}B_8O_{58}]^{24-}$ anionic network (c) in $Cd_{12}Ge_{17}B_8O_{58}$.

atoms are in oxidation states of +4, +3, and +2, respectively, based on our calculations.

The $Ge(2)O_4$, $Ge(3)O_4$, and $Ge(4)O_4$ tetrahedra and $Ge(5)O_6$ octahedra are interconnected via vertex sharing into a 1D $[Ge_4O_{12}]_n$ chain along the c axis (Figure 4a). Such chain is essentially identical to those in $Ca_{10}Ge_{16}B_6O_{51}$. Differently from those in $Ca_{10}Ge_{16}B_6O_{51}$, each 1D chain is connected with three neighboring ones via Ge(2)−O−Ge(2) and Ge(4)−O−Ge(4) bridges to form a 3D $[Ge_4O_{10.5}]_n$ network with small tunnels of 4-MR and large tunnels of 24-MR along the c axis (Figure 4b). Such Ge−O network could be also viewed to be built from 2D $[Ge_4O_{10.75}]_n$ layers observed in $Ca_{10}Ge_{16}B_6O_{51}$ via additional interlayer Ge−O−Ge connections. The different Ge−O skeletons formed in the above two compounds are mainly due to the different packing fashions of the $[Ge_4O_{10.75}]_n$ layers along the b axis. In $Ca_{10}Ge_{16}B_6O_{51}$, the two neighboring $[Ge_4O_{10.75}]_n$ layers are related to each other by shifting one-half of the a axis; hence, no direct interlayer Ge−O−Ge connections are formed. In $Cd_{12}Ge_{17}B_8O_{58}$, neighboring $[Ge_4O_{10.75}]_n$ layers are perfectly aligned along the b axis to allow formation of direct interlayer Ge−O−Ge bridges; hence, a 3D $[Ge_4O_{10.5}]_n$ network is formed. Every pair of $B(1)O_4$ and $B(2)O_4$ tetrahedra form a B_2O_7 dimer via vertex sharing, and four such B_2O_7 dimers are connected to a central $Ge(1)O_4$ by corner sharing into a $[Ge(B_2O_7)_4]^{28-}$ cluster (Figure 4c). Such $[Ge(B_2O_7)_4]^{28-}$ clusters are grafted into the above 24-MR tunnels of the $[Ge_4O_{10.5}]_n$ network via B−O−Ge bridges with 12-corner sharing, forming three types of small 1D tunnels of 5-, 6-, and 7-MR along the c axis in the 3D $[Ge_{17}B_8O_{58}]^{24-}$ anionic structure (Figure 4d). The 5-MR is composed of two GeO_4 and three BO_4, whereas the 6-MR contains one GeO_6, three GeO_4, and two BO_4. The 7-MR is formed by two GeO_6, four GeO_4, and one BO_4 groups. The B−O−B bond angle is 134.0(4)°, and the Ge−O−Ge and B−O−Ge angles are in the range of 119.6(1)−28.4(2)° and 116.5(3)−25.3(3)°, respectively. These bond angles are comparable to those previously reported in related borongermanates.[1−12] Cd(1), Cd(2), and Cd(3) cations are located at the 5-, 7-, and 6-MR tunnels, respectively (Figure 3b).

The most interesting aspect of the two structures is that both compounds are germanium rich rather than boron rich as in most metal borogermanates reported previously. Furthermore, they both exhibit 1D $[Ge_4O_{12}]_n$ chains consisting of pure Ge−O polyhedra, which is unique and different from other metal borogermanates reported previously. According to the atomic ratios of Ge/B (Table S2, Supporting Information), all metal

dx.doi.org/10.1021/ic2008254 |Inorg. Chem. 2011, 50, 8861–8868

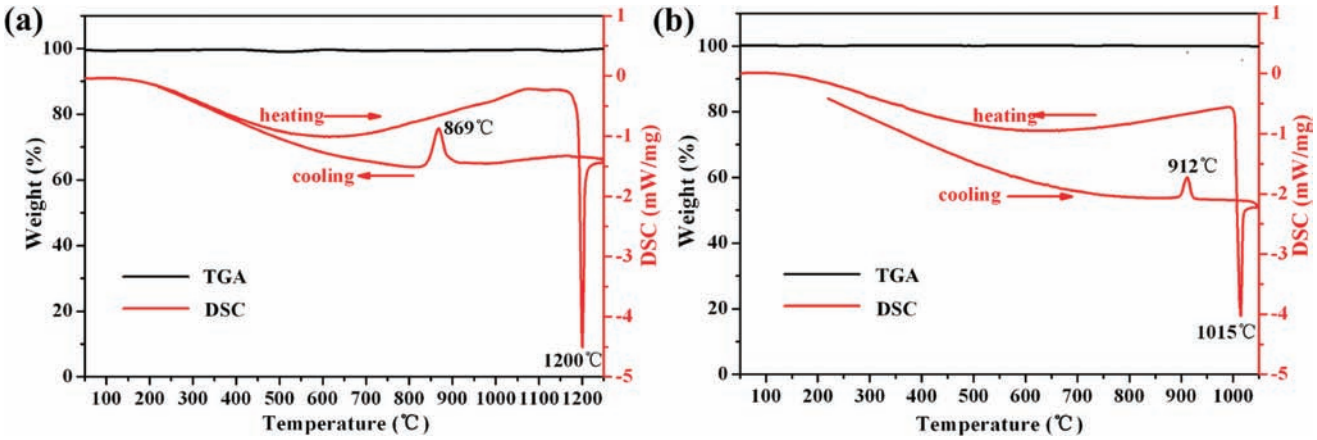

Figure 5. TGA and DSC curves of $Ca_{10}Ge_{16}B_6O_{51}$ (a) and $Cd_{12}Ge_{17}B_8O_{58}$ (b).

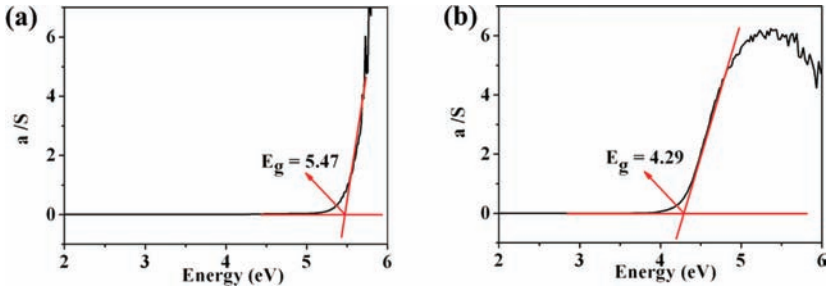

Figure 6. UV−vis diffuse reflectance spectrum of $Ca_{10}Ge_{16}B_6O_{51}$ (a) and $Cd_{12}Ge_{17}B_8O_{58}$ (b).

borogermanates reported can be derived into two types: boron rich with the Ge/B ratios smaller than or close to 1 and germanium rich with the ratios much larger than 1.[3−12] Most borogermanates belong to the first type, in which "isolated" GeO_4 tetrahedra connect with several boron oxide clusters such B_3O_7 in $CsGeB_3O_7$ and B_4O_9 in $K_2GeB_4O_9\cdot 2H_2O$, etc.[3,4] However, in the structure of the few germanium-rich compounds, Ge−O polyhedra can form various 1D chains which are further interconnected by "isolated" BO_4 tetrahedra. For instance, vertex-sharing GeO_4 tetrahedra form the infinite chains $[Ge_6O_{18}]_n$ in $NH_4[BGe_3O_8]$.[6b] Comparing the 1D gemanium oxide chains in $NH_4[BGe_3O_8]$ and those in our compounds, some differences are noticed. First, the $[Ge_6O_{18}]_n$ chain is built by pure GeO_4 tetrahedra whereas the $[Ge_4O_{12}]_n$ chains are based on both GeO_4 tetrahedra and GeO_6 octahedra. Second, the parallel $[Ge_6O_{18}]_n$ chains are connected by BO_4 tetrahedra in the structure of $NH_4[BGe_3O_8]$, but the $[Ge_4O_{12}]_n$ chain in our title compunds is directly fused with each other via a Ge−O−Ge bond into a 2D layer or 3D network. Hence, these two compounds are very unique in the chemistry of metal borogermanates.

A related 3D Ge−O framework can be found in $Cd_2Ge_7O_{16}$ as well as its isomorphic $Ca_2Ge_7O_{16}$.[18] Both $Cd_{12}Ge_{17}B_8O_{58}$ and $Cd_2Ge_7O_{16}$ feature 3D frameworks that are built up from 1D $[Ge_4O_{12}]_n$ chains composed of GeO_4 tetrahedra and GeO_6 octahedra. However, the connection fashions between these 1D chains are different, which resulted in formation of tunnels with different sizes. Each $[Ge_4O_{12}]_n$ chain is connected to three neighboring ones in $Cd_{12}Ge_{17}B_8O_{58}$. In $Cd_2Ge_7O_{16}$, each $[Ge_4O_{12}]_n$ chain is connected to five neighboring ones and only small 1D tunnels of 8-MR and 4-MR along the *c* axis are formed. Furthermore, interchain GeO_6−GeO_4−GeO_6 connections are also observed in addition to the GeO_6−GeO_4−GeO_4−GeO_6 connections. These structural differences are mainly due to the presence of BO_4 tetrahedra in $Cd_{12}Ge_{17}B_8O_{58}$. $Cd_2Ge_7O_{16}$ is isomorphic with $Ca_2Ge_7O_{16}$, whereas the structures of $Cd_{12}Ge_{17}B_8O_{58}$ and $Ca_{10}Ge_{16}B_6O_{51}$ are quite different. Hence, introduction of B atoms into the metal germinates may result in materials with a variety of new structures.

TGA and DSC Studies. TGA studies indicate no obvious weight loss before 1250 °C for $Ca_{10}Ge_{16}B_6O_{51}$ and 1050 °C for $Cd_{12}Ge_{17}B_8O_{58}$; hence, both compounds have a very high thermal stability (Figure 5), which is related with the absence of water or organic templates in their structures. DSC diagrams of $Ca_{10}Ge_{16}B_6O_{51}$ and $Cd_{12}Ge_{17}B_8O_{58}$ exhibit endothermic peaks at 1200 and 1015 °C in the heating curves and exothermic peaks at 869 and 912 °C in the cooling curves, respectively, indicating that they melt congruently at around 1200 and 1015 °C, respectively (Figure 5). These behaviors indicate that their single crystals with large size and high quality could be grown by the Czochralski method.

Optical Properties. The optical diffuse reflectance spectra revealed that both $Ca_{10}Ge_{16}B_6O_{51}$ and $Cd_{12}Ge_{17}B_8O_{58}$ are insulators with optical band gaps around 5.47 and 4.29 eV, respectively (Figure 6). The UV−vis−NIR absorption spectra of $Ca_{10}Ge_{16}B_6O_{51}$ and $Cd_{12}Ge_{17}B_8O_{58}$ show little absorption in the range of 300−2500 nm (Figure S5, Supporting Information), and their IR spectra exhibit very high transmittance in the range of 4000−1500 cm^{-1} (2.50−6.67 μm) (Figure S6, Supporting Information). Hence, $Ca_{10}Ge_{16}B_6O_{51}$ and $Cd_{12}Ge_{17}B_8O_{58}$ are transparent in the range of 0.30−6.67 μm.

dx.doi.org/10.1021/ic2008254 |*Inorg. Chem.* 2011, 50, 8861–8868

The IR spectra of $Ca_{10}Ge_{16}B_6O_{51}$ and $Cd_{12}Ge_{17}B_8O_{58}$ also display a series of strong absorption bands with frequency below 1200 cm^{-1} (Figure S6, Supporting Information). The intense absorption bands region at 1000−1200 cm^{-1} are due to the presence of the BO_4 tetrahedra, and the splitting of the bands into three peaks at 1180, 1148, and 1049 cm^{-1} for $Ca_{10}Ge_{16}B_6O_{51}$ and 1137, 1063, and 1023 cm^{-1} for $Cd_{12}Ge_{17}B_8O_{58}$ may be caused by the distortion of BO_4 tetrahedra from the ideal T_d symmetry which removes the degeneracy of the infrared active asymmetric stretching vibration.[19a] The symmetric stretching and asymmetric bending vibration of BO_4 tetrahedra is observed at 765 and 612 cm^{-1} for $Ca_{10}Ge_{16}B_6O_{51}$, respectively, and at 785 and 642 cm^{-1} for $Cd_{12}Ge_{17}B_8O_{58}$.[19b] The absorption bands at 877 and 730 cm^{-1} for $Ca_{10}Ge_{16}B_6O_{51}$ and at 887 and 709 cm^{-1} for $Cd_{12}Ge_{17}B_8O_{58}$ are typical for the stretch of Ge−O bonds from the GeO_4 tetrahedra and the GeO_6 octahedra, respectively.[19c] Since the bending modes of BO_4, GeO_4, and GeO_6 polyhedron are likely to be significantly intermixed within the low-frequency vibrations, the absorption with frequency below 600 cm^{-1} is very hard to be assigned in detail. The IR spectra suggest that the B atoms were present as BO_4 groups and Ge atoms appeared as GeO_4 and GeO_6 groups in both compounds, which is in good agreement with those of the structural analyses.

Since $Ca_{10}Ge_{16}B_6O_{51}$ and $Cd_{12}Ge_{17}B_8O_{58}$ are acentric structurally, therefore, they may exhibit SHG responses. SHG measurements on a Q-switched Nd:YAG laser with the sieved crystal samples (70−100 mesh) revealed that both of them display very weak SHG responses that are less than 0.1× KDP (KH_2PO_4). This is mainly originated from the distorted BO_4 tetrahedra present in the structures. According to anionic group theory, the overall SHG response of the crystal is the geometrical superposition of the microscopic second-order susceptibility.[20] Thus, the weak SHG responses of $Ca_{10}Ge_{16}B_6O_{51}$ and $Cd_{12}Ge_{17}B_8O_{58}$ are not surprising and could be mainly attributed to three factors. First, the BO_4 tetrahedron possesses only a small microscopic second-order susceptibility; second, the concentrations of BO_4 tetrahedra in the $Ca_{10}Ge_{16}B_6O_{51}$ and $Cd_{12}Ge_{17}B_8O_{58}$ are very low, and finally, the orientations of BO_4 tetrahedra make the polarizations of these groups largely cancel out each other. For instance, in the $Ca_{10}Ge_{16}B_6O_{51}$ structure, the B(2)−O(24) and B(3)−O(26) bonds are oriented toward the +c axis whereas the B(1)−O(23) bonds are toward the −c axis. These antiparallel arrangements of BO_4 tetrahedra along the c axis are unfavorable to produce a large macroscopic polarization, especially in the case of B(1)−O(23), B(2)−O(24), and B(3)−O(26) bonds which have the shortest B−O distances and correspond to the direction of polarization for the $B(1)O_4$, $B(2)O_4$, and $B(3)O_4$ tetrahedra, respectively.

CONCLUSIONS

In summary, two new borogermanates with noncentrosymmetric structures, namely, $Ca_{10}Ge_{16}B_6O_{51}$ and $Cd_{12}Ge_{17}B_8O_{58}$, have been prepared and structurally characterized. Interestingly, both of them contain the 1D $[Ge_4O_{12}]_n$ chain composed of GeO_4 tetrahedra and GeO_6 octahedra. These chains are condensed into a 2D $[Ge_4O_{10.75}]_n$ layer in $Ca_{10}Ge_{16}B_6O_{51}$ or a 3D $[Ge_4O_{10.5}]_n$ network in $Cd_{12}Ge_{17}B_8O_{58}$. These two different Ge−O skeletons are further decorated by BO_4 or/and B_2O_7 groups into two types of B−Ge−O frameworks. Both compounds are acentric structurally, but unfortunately their SHG responses are very weak. However, it is possible to enhance the SHG response of such materials by inclusion of more B−O groups, especially the BO_3 groups or introduction of the cations with a lone pair such as Pb^{2+} and Bi^{3+}. Our future research efforts will be devoted to the design and preparation of other alkaline-earth and transition-metal borogermanates, especially those of the boron-rich ones.

ASSOCIATED CONTENT

Supporting Information. X-ray crystallographic files in CIF format, simulated and measured XRD patterns, Rietveld refinement plots of XRD powder patterns, and UV−vis and IR spectra. This material is available free of charge via the Internet at http://pubs.acs.org.

AUTHOR INFORMATION

Corresponding Author

*Fax: (+86)591-83714946. E-mail: mjg@fjirsm.ac.cn.

ACKNOWLEDGMENT

This work was supported by the National Natural Science Foundation of China (Nos. 20731006, 20825104, 21001107, and 20821061) and Key Project of FJIRSM (No. SZD07001-2).

REFERENCES

(1) (a) Dadachov, M. S.; Sun, K.; Conradsson, T.; Zou, X.-D. *Angew. Chem., Int. Ed.* **2000**, *39*, 3674. (b) Li, Y.-F.; Zou, X.-D. *Acta Crystallogr.* **2003**, *C59*, 471. (c) Li, Y.-F.; Zou, X.-D. *Angew. Chem., Int. Ed.* **2005**, *44*, 2012.

(2) (a) Wang, G.-M.; Sun, Y.-Q.; Yang, G.-Y. *Cryst. Growth Des.* **2005**, *5*, 313. (b) Zhang, H.-X.; Zhang, J.; Zheng, S.-T.; Yang, G.-Y. *Inorg. Chem.* **2005**, *44*, 1166. (c) Pan, C.-Y.; Liu, G.-Z.; Zheng, S.-T.; Yang, G.-Y. *Chem.—Eur. J.* **2008**, *14*, 5057. (d) Cao, G.-J.; Fang, W.-H.; Zheng, S.-T.; Yang, G.-Y. *Inorg. Chem. Commun.* **2010**, *13*, 1047.

(3) (a) Lin, Z.-E.; Zhang, J.; Yang, G.-Y. *Inorg. Chem.* **2003**, *42*, 1797. (b) Zhang, H.-X.; Zhang, J.; Zheng, S.-T.; Wang, G.-M.; Yang, G.-Y. *Inorg. Chem.* **2004**, *43*, 6148.

(4) Kong, F.; Jiang, H.-L.; Hu, T.; Mao, J.-G. *Inorg. Chem.* **2008**, *47*, 10611.

(5) (a) Parise, J.-B.; Gier, T.-E. *Chem. Mater.* **1992**, *4*, 1065. (b) Ihara, M. *Yogyo Kyokai Shi* **1971**, *79*, 152.

(6) (a) Xiong, D.-B.; Zhao, J.-T.; Chen, H.-H.; Yang, X.-X. *Chem.—Eur. J.* **2007**, *13*, 9862. (b) Xiong, D.-B.; Chen, H.-H.; Li, M.-R.; Yang, X.-X.; Zhao, J.-T. *Inorg. Chem.* **2006**, *45*, 9301.

(7) Heymann, G.; Huppertz, H. *J. Solid State Chem.* **2006**, *179*, 370.

(8) (a) Zhang, J.-H.; Li, P.-X.; Mao, J.-G. *Dalton Trans* **2010**, *39*, 5301. (b) Zhang, J.-H.; Hu, C.-L.; Xu, X.; Kong, F.; Mao, J.-G. *Inorg. Chem.* **2011**, *50*, 1973.

(9) (a) Dzhurinskii, B. F.; Pobedina, A. B.; Palkina, K. K.; Komova, M. G. *Russ. J. Inorg. Chem.* **1998**, *43*, 1488. (b) Ilyukhin, A. B.; Dzhurinskii, B. F. *Russ. J. Inorg. Chem.* **1994**, *39*, 556. (c) Dzhurinskii, B. F.; Lysanova, G. V.; Komova, M. G.; Gokhman, L. Z.; Krut'ko, V. A. *Russ. J. Inorg. Chem.* **1995**, *40*, 1699. (d) Dzhurinskii, B. F.; Ilyukhin, A. B. *Russ. J. Inorg. Chem.* **2000**, *45*, 1. (e) Bandurkin, G. A.; Lysanova, G. V.; Palkina, K. K.; Krut'ko, V. A.; Komova, M. G. *Russ. J. Inorg. Chem.* **2004**, *49*, 213.

(10) (a) Kaminskii, A. A.; Mill, B. V.; Belokoneva, E. L.; Butashin, A. V. *Izv. Akad. Nauk SSSR, Neorg. Mater.* **1990**, *26*, 1105. (b) Belokoneva, E. L.; Mill, B. V.; Butashin, A. V.; Kaminskii, A. A. *Izv. Akad. Nauk SSSR, Neorg. Mater.* **1991**, *27*, 1700. (c) Lysanova, G. V.; Dzhurinskii, B. F.; Komova, M. G.; Tsaryuk, V. I.; Tananaev, I. V. *Inorg. Mater.* **1989**, *25*, 545. (d) Taibi, M.; Airde, J.; Boukhari, A. *Ann. Chim.-Sci. Mater.* **1998**, *23*, 285. (e) Belokoneva, E. L.; David, W. I. F.; Forsyth, J. B.; Knight, K. S. *J. Phys.: Condens. Matter* **1998**, *10*, 9975.

(11) Bluhm, K.; Mueller-Buschbaum, H. *J. Less Common Met.* **1989**, *147*, 133.
(12) Zhang, J.-H.; Kong, F.; Mao, J.-G. *Inorg. Chem.* **2011**, *50*, 3037.
(13) Wendlandt, W. M.; Hecht, H. G.*Reflectance Spectroscopy*; Interscience: New York, 1966.
(14) Kutz, S. K.; Perry, T. T. *J. Appl. Phys.* **1968**, *39*, 3798.
(15) (a) Larson, A. C.; Von Dreele, R. B. *Los Alamos National Laboratory Report LAUR* **1994**, 86–748. (b) Toby, B. H. *J. Appl. Crystallogr.* **2001**, *34*, 210.
(16) (a) *CrystalClear*, Version 1.3.5; Rigaku Corp.: Woodlands, TX, 1999. (b) Sheldrick, G. M. *SHELXTL, Crystallographic Software Package, SHELXTL*, Version 5.1; Bruker-AXS: Madison, WI, 1998. (c) Spek, A. L. *J. Appl. Crystallogr.* **2003**, *36*, 7.
(17) (a) Brown, I. D.; Altermatt, D. *Acta Crystallogr.* **1985**, *B41*, 244. (b) Brese, N. E.; O'Keeffe, M. *Acta Crystallogr.* **1991**, *B47*, 192.
(18) (a) Plattner, E.; Völlenkle, H. *Chem. Mon.* **1977**, *108*, 443. (b) Redhammer, J. G.; Roth, G.; Amthauer, G. *Acta Crystallogr.* **2007**, *C63*, i47.
(19) (a) Reshak, A. H.; Chen, X.-A.; Song, F.-P.; Kityk, I. V.; Auluck, S. *J. Phys.: Condens. Matter* **2009**, *21*, 205402. (b) Pan, S.-L.; Watkins, B.; Smit, J. P.; Marvel, M. R.; Saratovsky, I.; Poeppelmeier, K. R. *Inorg. Chem.* **2007**, *46*, 3851. (c) Rachkovskaya, G. E.; Zakharevich., G. B. *J. Appl. Spectrosc.* **2007**, *74*, 86.
(20) Chen, C.-T.; Ye, N.; Lin, J.; Jiang, J.; Zeng, W.-R.; Wu, B.-C. *Adv. Mater.* **1999**, *11*, 1071.